LIGHTWEIGHT DESIGN RESEARCH ON COMPOSITE FRAME OF ORCHARD CRAWLER VEHICLE BASED ON INTELLIGENT OPTIMIZATION METHOD

Dongwen GUO[1 1,2], Hongxian WANG [1,2], Jialin WANG [1,2], Weigang XUE [1,2], Xiaoguo WANG [1,2,*]

The double-layer composite frame of the new multifunctional orchard crawler vehicle has problems of excessive weight and strength redundancy, which affect operational mobility and energy efficiency. This study carried out 3D modeling and finite element analysis, selected 10 key parameters, and conducted parameter optimization by using the response surface model, Kriging surrogate model, and the Multi-Objective Seagull Optimization Algorithm. The results show that after optimization, the frame weight is reduced from 226.06 kg to 192.35 kg. Its maximum stress remains below the allowable stress, and the natural frequency avoids the resonance range, thus achieving the lightweight optimization goal.

Keywords: Composite frame of orchard crawler vehicle; Lightweight design; Sensitivity analysis; Multi-Objective Seagull Optimization Algorithm (MOSOA).

1. Introduction

With the accelerated shift of modern agriculture toward intelligence and precision, orchard crawler transporters have become a key part of smart agricultural equipment, playing an increasingly important role [1], [2], [3]. They can independently transport fruit and agricultural materials, greatly reduce labor intensity and improve work efficiency. However, most orchards in China are in hilly and mountainous areas with complex, rugged terrain, which poses severe challenges to the transporters' terrain crossing capacity, maneuverability, and endurance [4], [5]. Traditional frame design relies heavily on experience and analogy, leading to structural redundancy and low material utilization—resulting in an overweight frame [6] that severely limits the transporter's single-charge operation time and range [7], [8]. Therefore, lightweight optimization of the frame

[1] * Corresponding author, College of Agricultural Engineering, Shanxi Agricultural University, Taigu 030801, China; wxg315550@sxau.edu.cn

2 Dryland Farm Machinery Key Technology and Equipment Key Laboratory of Shanxi Province, Taigu 030801, China

(on the premise of meeting performance requirements) has become an essential and core technical approach to enhance the overall performance of orchard crawler transporters [9].

Structural optimization is the key technology for lightweight design. By using advanced mathematical, physical, and engineering methods, it redesigns the frame's topology, shape, and size to reduce weight [10], [11]. Researchers from Beijing Forestry University [12] used a multi-condition collaborative topology optimization method to reconstruct a crawler frame, reducing its weight by 124.5 kg (21.1%) while improving stiffness, strength, and collision resistance performance. Size optimization adjusts component cross-sections for rational material use: Wu et al. [13] reduced a mountain orchard wheeled transporter's frame weight by 12.4% by modifying crossbeam layout and reducing plate thickness, while meeting strength and stiffness requirements. Zhou et al. applied size optimization to lightweight a commercial vehicle frame using the NSGA-II algorithm, achieving a 12.24% weight reduction while satisfying fatigue life and performance requirements [14].

Optimization algorithms are mathematical tools that find optimal or near-optimal solutions under constraints through systematic search and iteration. Many studies have explored such algorithms: Xiu [15] applied the multi-objective particle swarm optimization algorithm to reduce carriage weight by 31.5%. However, these algorithms often converge slowly and easily fall into local optima—problems the Seagull Optimization Algorithm (SOA) addresses effectively. Pathak et al. [16] systematically reviewed the principles, improvement strategies and engineering applications of the Seagull Optimization Algorithm (SOA) and its variants, providing core theoretical references and application guidance for applying this intelligent algorithm to solve various complex optimization problems. Liu et al. [17] used NSGA-II to obtain Pareto solutions for moving-plate lightweight optimization and adopted interval vague set decision to select the optimal scheme. Gaurav et al. proposed the Multi-Objective Seagull Optimization Algorithm (MOSOA) integrated with dynamic archive and roulette wheel selection, which outperforms existing meta-heuristic algorithms validated by 24 benchmark functions and 6 constrained engineering design problems [18].

Previously, most orchard vehicles in lightweight studies were wheeled, but their application was limited by uneven roads, large slope variations and complex operational environments. This study focuses on lightweight design of a new hybrid oil-electric tracked orchard vehicle: its tracked traveling mechanism ensures complex terrain adaptability, and the composite frame supports multi-functional operations. By combining SolidWorks and ANSYS, parametric modeling and finite element analysis of the frame were conducted, followed by correlation and sensitivity analysis of parameters.

A Kriging surrogate model was constructed, and the optimal solution was screened via the Multi-Objective Seagull Optimization Algorithm (MOSOA) to achieve the lightweight goal.

2. Optimization Objectives and Process of the Crawler Vehicle Frame

2.1 Optimization Objectives of the Crawler Vehicle Frame

Optimization design is a process that improves the efficiency, rationality and demand-adaptability of a design by adjusting schemes and modifying parameters on the premise of satisfying functional requirements and constraints.

This study focuses on the lightweight design of a new type of hybrid oil-electric orchard crawler transporter. The frame model is presented in Fig. 1, and the material properties (Q235: The main international equivalents of Q235 steel are EN S235JR, ASTM A36, and JIS SS400.) are listed in Table 1.

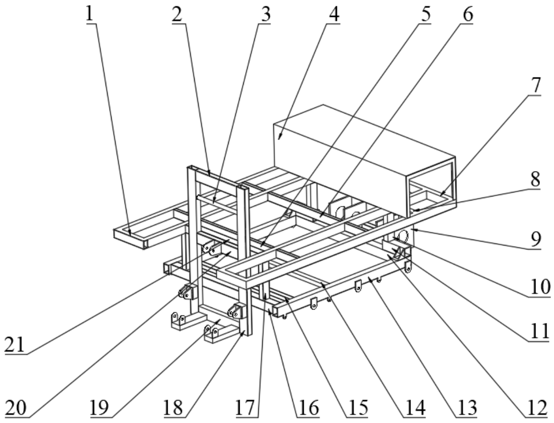

Fig. 1. Frame Structure Schematic
1. U-shaped beam; 2. Upper crossbeam of traction frame; 3. Traction rod; 4. Partition plate; 5. Middle crossbeam I; 6. Middle crossbeam II; 7. Rear crossbeam I; 8. Middle crossbeam III; 9. Rectangular plate; 10. Rear support beam I; 11. Rear support beam II; 12. Rear crossbeam II; 13. Longitudinal beam; 14. Lower-middle crossbeam II; 15. Lower-middle crossbeam I; 16. Front crossbeam I; 17. Front support beam; 18. Longitudinal beam of traction frame; 19. Lower crossbeam of traction frame; 20. Middle crossbeam of traction frame; 21. Front crossbeam I

Table 1

Parameters of the Tracked Vehicle Frame Model

Material	Density (kg/m³)	Thermal Expansion Coefficient (1/°C)	Young's Modulus (GPa)	Poisson's Ratio	Bulk Modulus (Pa)	Shear Modulus (Pa)
Q235	7850	1.18×10^{-5}	210	0.3	1.75×10^{11}	8.08×10^{10}

2.2 Steps for Lightweight Design of Crawler Vehicle Frame

The flowchart of all optimization steps is shown in Fig. 2.

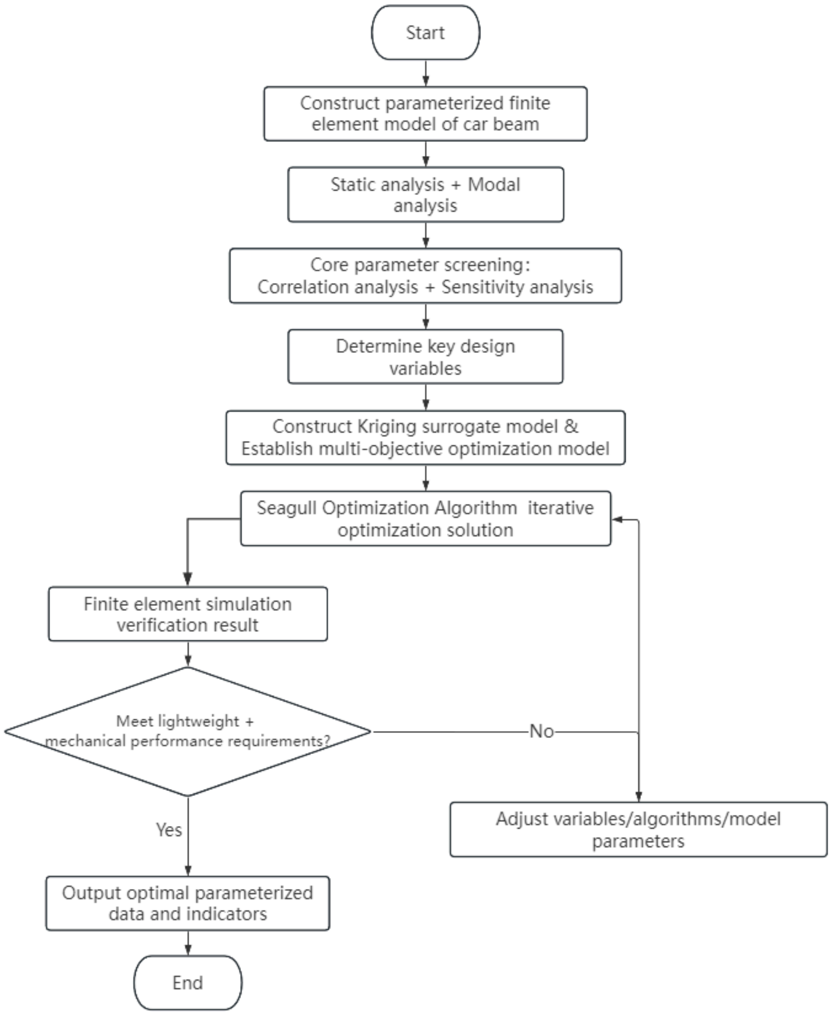

Fig. 2. Optimized Design Process

3 Mechanical Structure Analysis

3.1 Preliminary Preparation

Based on the simplification method in Ref. [19], we removed parts with little impact on frame finite element analysis and omitted tiny manufacturing structures to acquire more reliable results. The simplified frame model is displayed in Fig. 3. The geometric model was imported into ANSYS for finite element analysis. After mesh sensitivity tests, a uniform global mesh size of 5 mm was selected to balance calculation accuracy and efficiency.

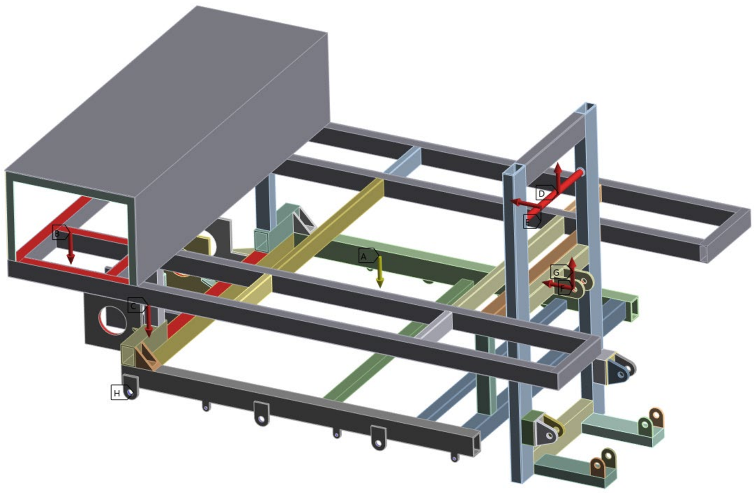

Fig. 3. Simplified Chassis Frame Model with Boundary Load Conditions

The frame of the crawler vehicle is made of Q235 steel, with a yield strength $\sigma_s = 235$ MPa. A safety factor n = 1.2 is adopted, and the equation for allowable stress is as follows:

$$[\sigma] = \frac{\sigma_S}{n} \tag{3}$$

where: $[\sigma]$ is the allowable stress, in MPa; σ_s is the yield strength of the material, in MPa; n is the safety factor. The allowable stress of the material is calculated as $[\sigma]$=195 MPa.

3.2 Static Structural Analysis

Static structural analysis was performed on the orchard crawler frame. Applied external loads included 1960 N from the implement, 784 N from the range extender, 1176 N total from two reducers, 119.56 N from the fuel tank, 588 N from the battery pack, and 588 N total from two motors.

Fixed constraints were set on the main frame's bottom support, and gravity was applied to the whole structure. Static analysis yielded the frame's maximum stress and maximum equivalent elastic strain distribution plots (Fig. 4). Results: max stress 133.32 MPa, max equivalent elastic strain 0.000634 mm. This stress was far below Q235 steel's allowable 195 MPa, confirming sufficient frame strength. Most frame areas had low stress and ample margin for optimization to improve material utilization.

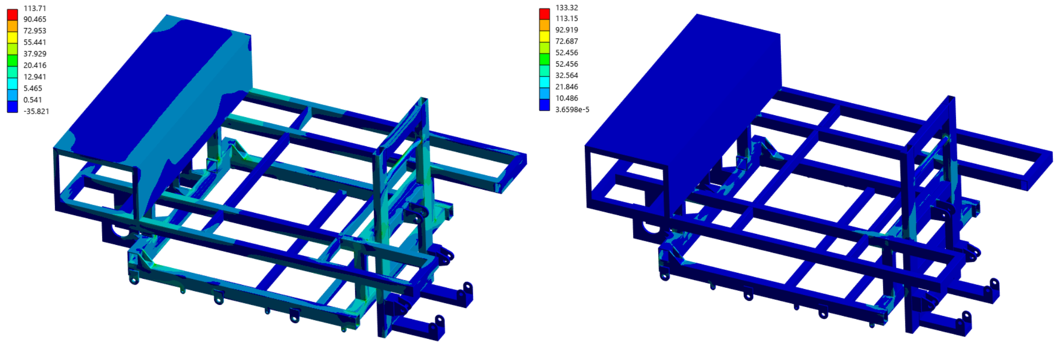

a. Orchard Tracked Vehicle Frame Maximum Principal Stress Cloud Map

b. Orchard Tracked Vehicle Frame Equivalent Stress Cloud Map

Fig. 4. Cloud Maps Related to Static Structural Analysis Results

3.3 Mode Analysis

Free modal analysis can reflect the inherent dynamic characteristics of the structure. Its analysis results are only related to material constitutive parameters and thus feature stronger universality. For this reason, this method was adopted in the present study [20].

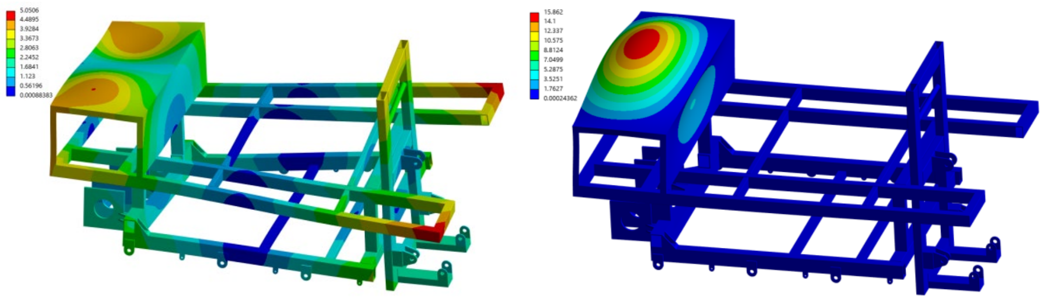

a. 7th-Order Mode Shape Cloud Map

b. 8th-Order Mode Shape Cloud Map

Fig.5. Mode Shape Cloud Maps of Frame from 7th to 8th Order

Since low-order modes contribute the most to the system response, the actual analysis focused on the 7th to 15th-order modes. Fig. 5 shows the 7th to 8th order mode shape distribution plots of the composite frame for the orchard crawler transporter, with the remaining mode shape distribution plots presented in Appendix A. The results of modal analysis are shown in Table 2.

Table 2

Mode Shapes of Tracked Vehicle Frame from 7th to 15th Order

Order	Modal frequency (Hz)	Amplitude (mm)	Main Vibration Location
7	40.032	5.0512	Frame composite torsion around X-axis and Z-axis

8	43.034	15.862	Rear bulkhead upward bending
9	56.652	6.9743	Rear frame rightward displacement
10	61.476	14.568	Rear frame torsion around X-axis
11	63.754	7.5648	Frame composite torsion around X-axis and Y-axis
12	70.751	7.4885	Frame torsion around Z-axis
13	83.83	17.634	Bulkhead multi-peak bending
14	88.851	21.535	Frame composite torsion around Z-axis and Y-axis
15	88.868	9.6376	Torsion between the bulkhead and the frame bottom

The main excitation sources of the frame of the orchard crawler vehicle studied in this study include the terrain impact excitation frequency ranging from 0 to 13.9 Hz, the meshing excitation frequency of the crawler wheel set ranging from 10 to 15 Hz, and the natural frequency of the mass without suspension ranging from 6 to 15 Hz. The power system is mainly driven by the vibration excitation of the drive motor. The motor used in this vehicle model is a YP100B5-48V2.2-1500 no carbon brush DC motor, and the vibration frequency caused by it can be calculated by equation (2).

$$F = \frac{N}{60} \tag{2}$$

where: N is the motor speed. According to equation (2), the idle excitation frequency can be calculated as 25 Hz. In summary, the frame studied in this subject is required to have low-order frequencies above 15 Hz while avoiding the motor idle frequency of 25 Hz. By comparing the calculation results with the modal analysis results, it can be seen that the main excitation frequencies do not overlap with the natural frequencies, and thus resonance will not occur.

4. Correlation and Sensitivity Analysis of Crawler Vehicle Frame

4.1 Selection of Key Parameters

Based on the multi-dimensional screening principle centered on structural relevance, 33 core structural parameters were sorted out in the initial design stage of the crawler vehicle frame (See Appendix D).

Aiming at continuous structural parameters in this research, the Pearson product-moment correlation coefficient (with a value range of [-1, 1]) was adopted to quantify the strength and direction of linear correlations, as presented in equation (3):

$$r_{xy} = \frac{\sum_{i=1}^{n}(x_i - \bar{x})(y_i - \bar{y})}{\sqrt{\sum_{i=1}^{n}(x_i - \bar{x})^2}\sqrt{\sum_{i=1}^{n}(y_i - \bar{y})^2}} \tag{3}$$

where: x_i and y_i are the sample data of the two variables; $\bar{x}$ and $\bar{y}$ are the sample means. Referring to the general standards for mechanical optimization, the screening thresholds are defined as follows: $|r_{\text{xy}}| \geq 0.7$ indicates a strong correlation; $0.3 \leq |r_{xy}| < 0.7$ indicates a moderate correlation; $|r_{\text{xy}}| < 0.3$ indicates a weak correlation or no correlation.

According to the engineering screening criteria, a preliminary screening was conducted after the correlation analysis of all variables, and the results are shown in Table 3 (The definitions of the codes are detailed in Appendix C).

Table 3

Initial Variable Screening

Correlation Category	Code
Strong Correlation	D、L2、T5、T6、W1、W4
Moderate Correlation	L4、L6、L9、T1、T2、T3、T11、T12、T17、W2、W3
Weak Correlation	L1、L5、L7、T4、T7、T8、T9、T10、T13、T14、T15、T16、T18、W5

4.2 Sensitivity Analysis

Sensitivity analysis is a quantitative analytical method for evaluating the response degree of model outputs to changes in input parameters.

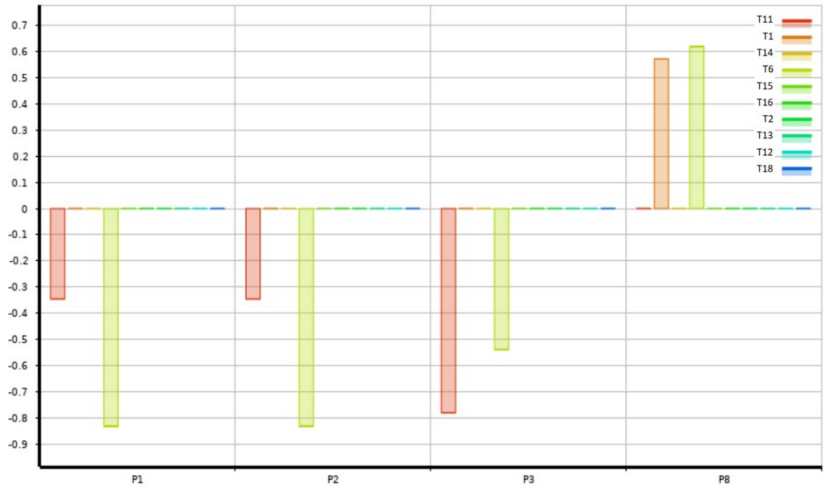

Fig. 6. Sensitivity Histogram

In this study, Latin Hypercube Sampling (LHS) was adopted to generate uniformly distributed sample points, and ANSYS Workbench was used to obtain the core performance indicators of each sample point. The relationship between optimization objectives and design parameters can be observed from the results. Fig. 6 shows partial results of the sensitivity analysis. The abscissa labels P1-Stress, P2-Strain, P3-Deformation, and P4-Mass in the figure represent the structural stress in MPa, the material strain (dimensionless or mm/mm), the structural deformation displacement in mm, and the structural mass in kg, respectively. These are the core performance indicators for finite element analysis, and the height and sign of each bar reflect the sensitivity of each design variable to these indicators. With the complete results presented in Appendix B. The optimized value ranges of each design variable for the frame are listed in Table 4.

Table 4

Value Range of Design Variables

Serial Number	Code	Original Value of Variable (mm)	Value Range	
			Lower Limit (mm)	Upper Limit (mm)
X1	D	27	23	31
X2	T1	4	2	6
X3	T3	5	3	7
X4	T17	4	2	6
X5	L4	70	60	80
X6	W3	70	60	80
X7	T6	4	2	6
X8	L2	60	50	70
X9	W1	79	70	87
X10	L5	40	30	50

4.3 Multi-objective Optimization Modeling of the Frame

The multi-objective optimization of the frame in this study takes lightweight design + mechanical performance guarantee as the core. The design variables are determined as the ten screened structural parameters $X_1 \sim X_{10}$ (denoted as $X = (X_1, X_2, \dots, X_{10})$), and the value of each variable shall satisfy the production specification constraints $X_L \leq X_i \leq X_U$ (where X_L and X_U are the lower and upper limits of the variables, respectively; refer to Table 4 for specific ranges).

The constraint functions focus on mass and stress: the mass constraint requires that the optimized frame mass M shall be no more than the original mass of 226.06 kg; the stress constraint specifies that the maximum equivalent stress σ_{max} of the frame made of Q235 steel under the extreme torsion condition shall not exceed 195 MPa. The objective functions are to minimize the frame mass M(X), maximum deformation $\delta_{max}(X)$ and maximum equivalent stress $\sigma_{max}(X)$, based on which the multi-objective optimization model is constructed. Accordingly, the multi-objective mathematical optimization model for the orchard crawler vehicle frame is established in equation (4):

$$\begin{cases} Find: & \boldsymbol{X} = (X_1, X_2, X_3, X_4, X_5, X_6, X_7, X_8, X_9, X_{10}) \\ & X_L \leq X_i \leq X_U \\ Min: & M = M(\boldsymbol{X}) \\ Min: & \delta = \delta_{\max}(\boldsymbol{X}) \\ Min: & \sigma = \sigma_{\max}(\boldsymbol{X}) \\ s.t.: & M \leq 226.06kg \\ & \sigma_{\max} \leq 195MPa \end{cases} \tag{4}$$

5. Lightweight Design of Frame Based on Kriging Surrogate Model

In the lightweight optimization of the frame, direct simulation iteration is extremely time-consuming. Meanwhile, the standalone application of the Multi-Objective Seagull Optimization Algorithm (MOSOA) leads to a large deviation between the optimization results and engineering practice due to the lack of simulation data support, making it difficult to meet the requirements. For this reason, the Kriging surrogate model is introduced.

5.1 Design of Experiments

Design of Experiments (DOE) is a method for scientifically planning the processes of sample selection, variable control, and data collection, with the purpose of acquiring reliable data to support analysis or modeling. The Latin Hypercube Sampling (LHS) design is adopted in this optimization design, which features uniform sampling distribution, strong coverage, and high efficiency in capturing variable space information.

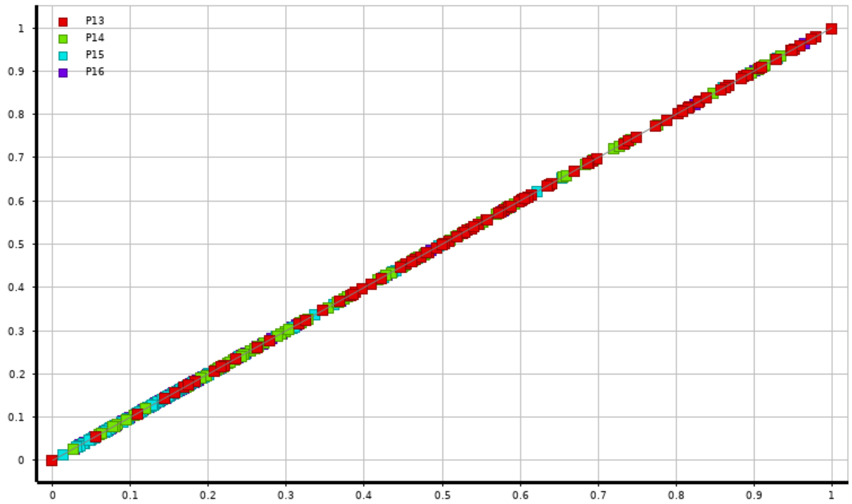

Fig. 7. Output the goodness-of-fit curve

The fitting curves between the output parameters are shown in Fig. 7. It can be seen that the output parameters, namely mass P13, maximum deformation P14, equivalent elastic strain P15, and maximum equivalent stress P16, are almost distributed on a single line, indicating that the sample points and various settings of the aforementioned Design of Experiments are very reasonable.

5.2 Multi-objective Optimization Based on the Seagull Optimization Algorithm

To address the technical demand for the collaborative optimization of structural performance and lightweight design of orchard tracked vehicles, this study introduces the Seagull Optimization Algorithm (SOA) to carry out multi-objective optimization design. Precise upgrading of the tracked vehicle structure is achieved through algorithm iteration, which provides a theoretical basis and technical approaches for the structural optimization of modern agricultural machinery.

5.2.1 Optimization Principle and Method

The Seagull Optimization Algorithm (SOA) is an intelligent optimization algorithm that simulates the natural behaviors of seagulls, including social migration, collaborative collision avoidance, and spiral attack [16].

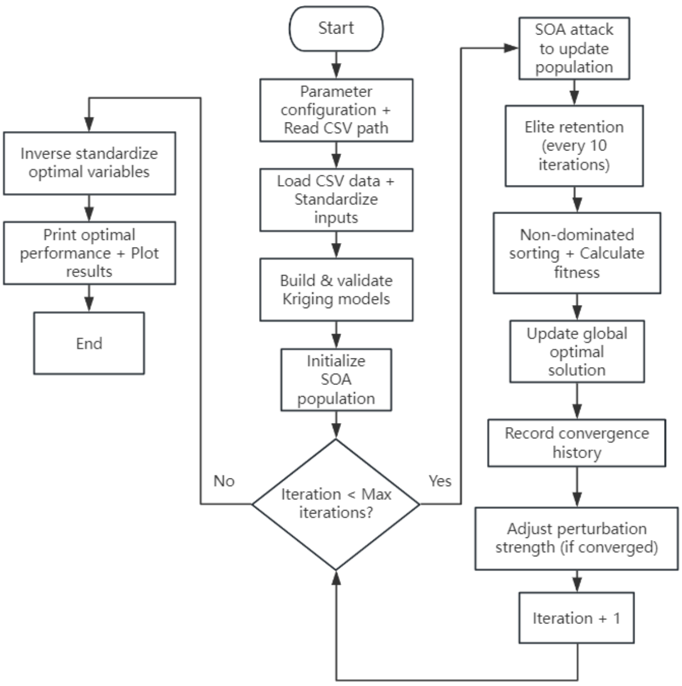

Fig. 8. Flowchart of SOA Algorithm's Iterative Convergence

The iterative flow chart of the MOSOA algorithm is shown in Fig. 8. Finite element and modal simulations were conducted in ANSYS Workbench; the sample dataset for establishing the Kriging surrogate model was exported from ANSYS in CSV format, preprocessed in Microsoft Excel, and then imported into PyCharm (Python) for surrogate model construction and seagull algorithm-based optimization.

5.2.2 Optimization Results

In this study, the multi-objective seagull optimization algorithm with a population size of 120 and maximum iterations of 200 achieves fast optimization and stable convergence. The frame mass is reduced from 226.06 kg to 192.35 kg, and the fitness stabilizes at the global optimum, with stress, deformation and other indicators meeting the design requirements.

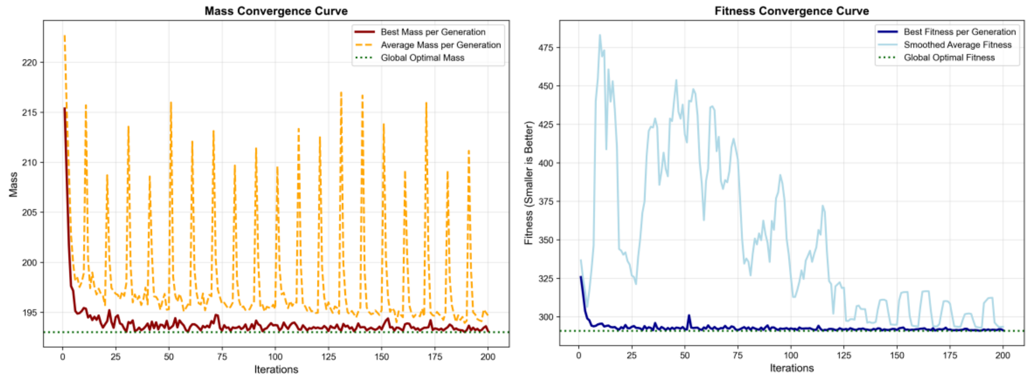

a Mass Convergence Curve b Fitness Convergence Curve

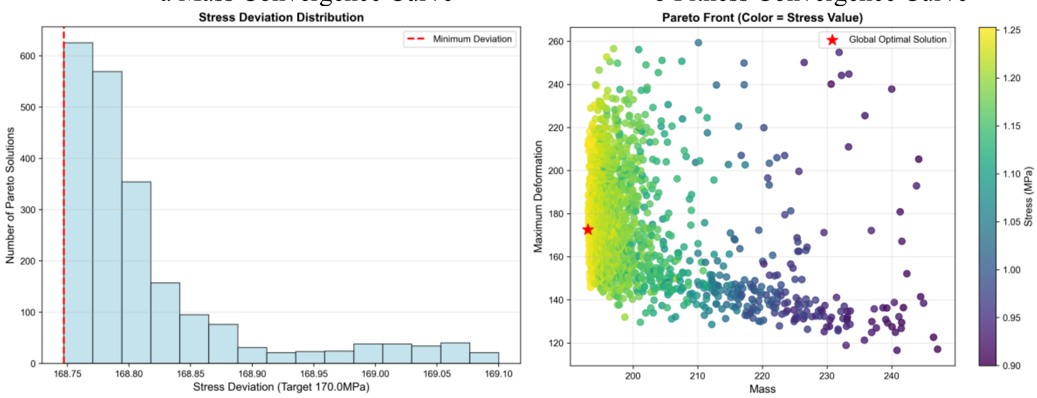

c. Stress Deviation Distribution Diagram d. Pareto Front Plot

Fig. 9. Diagrams Related to Optimization Results

Fig. 9 shows the charts related to the optimization results. It can be seen that the Pareto optimal solutions obtained in this study are uniformly distributed, and the global optimal solution can achieve a balance among multiple performance indicators. Combined with normalization and response surface analysis, the effectiveness of the optimal design scheme for the orchard crawler vehicle frame is verified.

Table 5

Response Value vs. Simulation Value Comparison Table

Comparison Indicator	Mass (kg)	Stress (MPa)	Deformation (mm)
Before Optimization	226.06	133.32	0.966
Response Value	193.36	169.95	1.345
Simulation Value	192.35	172.48	1.386
Error Rate	0.52%	1.49%	3.05%

To verify the error between the response values and the simulation values, simulations were carried out according to the optimized parameters, and the comparison between the response values and the simulation values is shown in Table 5.In this study, through Kriging-SOA multi-objective optimization, a mass reduction of more than 10% for the frame is achieved under the constraint of stress $\leqslant$ 195 MPa. Finally, the optimal values of the 10 design variables are determined from the Pareto optimal solutions, as shown in Table 6.

Table 6

Dimension values before and after optimization

Variable Name	Before optimization (mm)	After optimization (mm)	Rounded value (mm)
X1	27.00	23.19	23.00
X2	4.00	2.02	2.00
X3	5.00	3.02	3.00
X4	4.00	2.04	2.00
X5	70.00	60.10	60.00
X6	60.00	50.00	50.00
X7	4.00	2.02	2.00
X8	60.00	50.10	50.00
X9	79.00	70.23	70.00
X10	40.00	30.20	30.00

Based on the fourth strength theory, with the equivalent stress as the criterion for judging material yield failure and the maximum principal stress as the auxiliary standard, the structure was optimized. The results show that both the equivalent stress and the maximum principal stress after optimization are lower than the allowable stress. The errors between the response surface analysis results and the simulation values are within a reasonable range.

Compared with the pre-optimization parameters, the frame mass is reduced from 226.06 kg to 192.35 kg, with a lightweight rate of 14.91%. The stress and deformation are adjusted to 172.48 MPa and 1.386 mm respectively, both meeting the design constraints. The modal frequencies avoid the main excitation frequencies, eliminating the risk of resonance. The stress distribution of the optimized static structure is shown in Figures 10 and 11. The natural frequencies of the optimized orchard tracked vehicle frame are shown in Table 7.

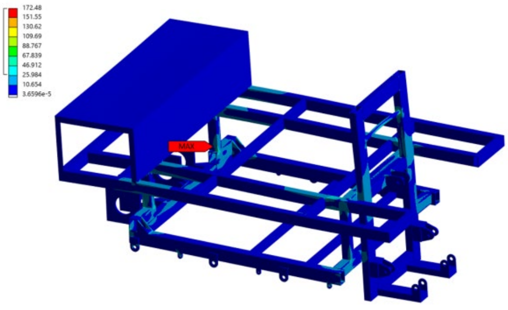

Fig. 10 Equivalent stress cloud map of the orchard crawler vehicle frame after optimization (deformation magnified 40x)

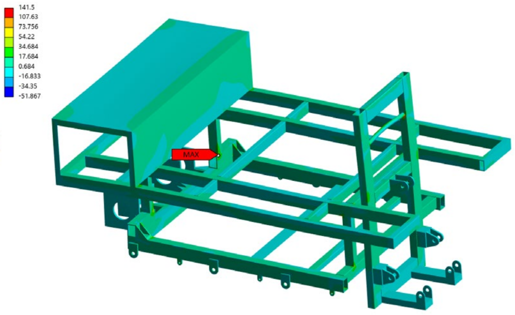

Fig. 11 Maximum principal stress cloud map of the optimized orchard crawler frame (deformation magnified 40x)

Table 7

Intrinsic frequencies of the optimized orchard crawler frame

Order	7	8	9	10	11	12	13	14	15
Modal frequency (Hz)	36.763	42.485	50.036	57.182	61.743	61.756	80.05	83.219	87.535

6. Conclusion

(1) Focusing on the frame of a new tracked hybrid oil-electric vehicle, this study establishes a multi-objective optimization model and adopts an intelligent optimization method combining the Kriging surrogate model and the multi-objective Seagull Optimization Algorithm (MOSOA) to achieve lightweight design.

(2) Based on field survey data, a finite element model of the frame is constructed, with static structural and free modal analyses completed. A two-stage "correlation analysis—sensitivity analysis" variable screening strategy eliminates redundant and weakly influential parameters, reducing optimization complexity. The Kriging model boosts computational efficiency, while the MOSOA balances global exploration and local exploitation for rapid convergence to Pareto-optimal solutions, verifying the method's scientific rationality and practicability

(3) Lightweight optimization achieves remarkable results: frame mass decreases from 226.06 kg to 192.35 kg (14.91% reduction). Post-optimization

maximum stress (172.48 MPa) and deformation (1.386 mm) are below Q235 steel's allowable stress (195 MPa) and design thresholds. Despite adjusted 7th–15th order modal frequencies, main excitation frequencies are avoided, eliminating resonance risks. Efficient weight reduction is realized while ensuring frame strength, stiffness, and dynamic performance.

The free-free modal analysis in this study only extracts natural frequencies, mode shapes, and vibration amplitudes, without calculating mode participation factors per axis and equivalent modal mass. These parameters can better reflect the directional contribution of each vibration mode, and will be further supplemented and analyzed in future research to improve the comprehensiveness of dynamic performance evaluation.

Addressing tracked orchard vehicles, complex terrain adaptability, this study resolves traditional frames, structural redundancy and high energy consumption, providing theoretical and technical support for lightweight design of hilly mountainous orchard equipment. Subsequent orchard operation experiments will measure frame off-road passing performance and reliability under complex conditions to further verify the lightweight effect.

Acknowledgement

This work was supported by the Science and Technology Innovation Enhancement Project of Shanxi Agricultural University (Project No. CXGC202412), the Special Project for Discipline Construction of Agricultural Engineering at Shanxi Agricultural University and the Key Project of the Key Research Program of Shanxi Province (Grant No. 202102020101012).

REFERENCES

[1] *J. Q. Liu,* Design and Optimization of the Frame for Orchard Picking Operation Platform, PhD Thesis, Shandong Jiaotong University, 2023.

[2] *D. G. Koc, M. Vatandas,* Development and performance analysis of an autonomous agricultural crawler vehicle for fruit transportation, Journal of Field Robotics, Vol. 42, Iss. 7, 2025, pp. 3189–3212.

[3] *S. L. Waslander, J. Kim,* Performance evaluation of an autonomously driven rubber-tracked vehicle in complex orchard terrain, Sensors, Vol. 22, Iss. 1, 2022, pp. 347, DOI: 10.3390/s22010347.

[4] *O. C. Barawid, A. Mizushima, N. Noguchi,* Development of an autonomous navigation system using a two-dimensional laser scanner for orchard crawlers, Computers and Electronics in Agriculture, Vol. 57, Iss. 1, 2007, pp. 1–10.

[5] *J. Miao,* Research on Lightweight Design of Chassis Frame Structure for Agricultural Machinery and Equipment, Southern Agricultural Machinery, Vol. 55, Iss. 08, 2024, pp. 156-157+183.

[6] *C. H. Zhou,* Design and Mechanical Analysis of Frame Structure for New Agricultural Crane, Southern Agricultural Machinery, Vol. 56, Iss. 15, 2025, pp. 121-123.

[7] *J. H. Wu, J. F. Chen, Y. H. Yang,* Design and Verification of Adaptive Leveling Control for Intelligent Chassis of Hilly Tracked Vehicle, Journal of Agricultural Mechanization Research, Vol. unmarked, Iss. unmarked, online 2025, pp. 1-9, URL: https://link.cnki.net/urlid/23.1233.S.20250915.1439.003.

[8] *G. David, S. Carsten, D. Berend,* Lightweight Design in Agricultural Machinery - CFRP Chassis for Forage Harvesters, ATZheavy duty worldwide, Vol. 17, Iss. 1, 2024, pp. 32-37.

[9] *K. Sookchanchai, S. Olarnrithinun, V. Uthaisangsuk,* Lightweight design of an automotive lower control arm using topology optimization for forming process, IOP Conference Series: Materials Science and Engineering, Vol. 1157, Iss. 1, 2021.

[10] *D. Gonçalves, J. Lopes, R. Campilho, J. Belinha,* An evolutionary structural optimization algorithm for the analysis of light automobile parts using a meshless technique, Engineering Computations, Vol. 39, Iss. 6, 2022, pp. 2081-2107.

[11] *P. Stabile, F. Ballo, M. Gobbi, G. Previati,* Multi-objective structural optimization of vehicle wheels: a method for preliminary design, Optimization and Engineering, Vol. 25, Iss. 2, 2023, pp. 1025-1050, DOI: 10.1007/S11081-023-09833-9.

[12] *Z. Q. Wang,* Lightweight Design of an Unmanned Vehicle Frame Based on Multi-condition Collaborative Optimization, PhD Thesis, Beijing Forestry University, 2020.

[13] *W. B. Wu, J. W. Liao, T. S. Hong,* Structural Analysis and Optimization of Frame for Mountain Orchard Wheeled Transporter, Transactions of the Chinese Society of Agricultural Engineering, Vol. 32, Iss. 11, 2016, pp. 39-47.

[14] *Z. W. Zhou, L. Shuai, C. Z. Xiang,* Research on Lightweight Design and Fatigue Life Optimization of a Commercial Vehicle Frame, Transportation Research Record, Vol. 2680, Iss. 2, 2026, pp. 453-474.

[15] *R. X. Xiu, C. Miao, X. H. Niu,* Optimal Design of Carriage Structure Based on Multi-objective Particle Swarm Optimization Algorithm, Engineering Machinery Abstracts, Vol. unmarked, Iss. 04, 2025, pp. 4-7.

[16] *V. K. Pathak, S. Gangwar, M. K. Dikshit,* A Comprehensive Survey on Seagull Optimization Algorithm and Its Variants, Archives of Computational Methods in Engineering, Vol. 32, Iss. 6, 2025, pp. 1-35, DOI: 10.1007/S11831-025-10249-0.

[17] *L. Liu, Z. Zhang, G. Li, N. Fu, X. Chen,* Lightweight design of moving-plate for injection moulding machine based on multi-objective optimization scheme mining, U.P.B. Sci. Bull., Series D, Vol. **86**, Iss. 1, 2024, pp. 3-16.

[18] *D. Gaurav, S. Kant, S. Mukesh,* MOSOA: A new multi-objective seagull optimization algorithm, Expert Systems with Applications, prepublish, Iss. unmarked, 2020, pp. 114150.

[19] *Y. Han,* Finite Element Analysis and Optimization Design of Light-Duty Truck Frame, PhD Thesis, Dalian Jiaotong University, 2019.

[20] *X. S. Liao, C. C. Bao,* Structural Optimization Design of UAV Wing Based on Response Surface Methodology, Journal of Mechanical Design, Vol. 42, Iss. S2, 2025, pp. 9-14.